



Contents lists available at ScienceDirect

Spectrochimica Acta Part A: Molecular and Biomolecular Spectroscopy

journal homepage: www.elsevier.com/locate/saa

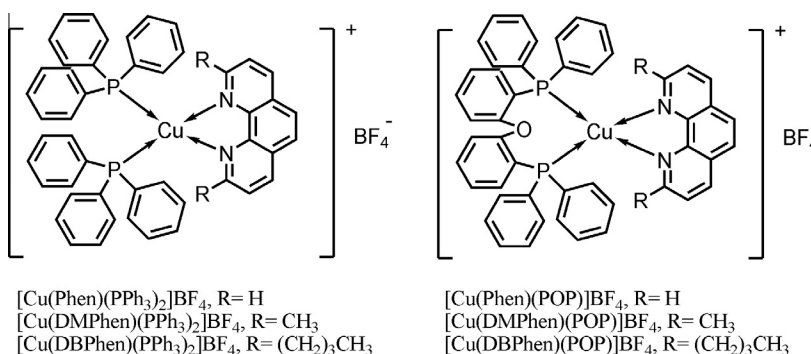
Synthesis and study on a series of phosphorescent Cu(I) complexes having sterically blocking ligands

Kai Zhang^{a,*}, Dong Zhang^b^a Correction Department of Education, The Central Institute for Correctional Police, Baoding 071000, China^b Institute of Penology, The Central Institute for Correctional Police, Baoding 071000, China

HIGHLIGHTS

- Six phosphorescent Cu(I) complexes were synthesized.
- Alkyl groups were introduced into 2,9-positions of 1,10-phenanthroline.
- Crystal structures, photophysical properties, and electronic nature were studied.
- The correlation between emission performance and alkyl group was investigated.

GRAPHICAL ABSTRACT



ARTICLE INFO

Article history:

Received 21 November 2013

Received in revised form 2 January 2014

Accepted 8 January 2014

Available online 18 January 2014

Keywords:

Cu(I) complexes
 Single crystal
 Steric hindrance
 Luminescence

ABSTRACT

In this paper, we report six phosphorescent Cu(I) complexes with 1,10-phenanthroline-derived ligands and phosphorous ligands, including their synthesis, crystal structures, photophysical properties, and electronic nature. The Cu(I) center has a distorted tetrahedral geometry within the Cu(I) complexes. Theoretical calculation reveals that all emissions originate from triplet metal-to-ligand-charge-transfer excited state. It is found that the introduction of alkyl moieties into 2,9-positions of 1,10-phenanthroline is highly effective on restricting the geometric relaxation that occurs in excited states, which greatly enhances the photoluminescence (PL) performances, including PL quantum yield improvement, PL decay lifetime increase, and emission blue shift.

© 2014 Elsevier B.V. All rights reserved.

Introduction

Recently, the design and synthesis of luminescent transition metal complexes have been sparked owing to their potential application in organoelectronic field such as chemosensors, display materials, biosensors, and solar-energy conversion dyes [1–2]. Most of research efforts focus on expensive metal complexes of Ir, Pt, Re, and Ru. On the other hand, there is also a strong need to replace the expensive functional materials with cheap ones,

which initiates a continuous progress in the design and synthesis of luminescent functional materials based on the first-row transition metal complexes. Luminescent Cu(I) complexes have drawn much attention owing to their promising performance as optoelectrical material, as well as their advantages of low toxicity, low cost, and redundant resource. Many luminescent Cu(I) complexes have been reported and discussed, and the correlation between molecular structure and photophysical performance is also fully investigated [3,4].

As for a typical Cu(I) complex with d^{10} system, the ground state adopts a tetrahedral coordination geometry, while the excited state tries to transfer to a tetragonally flattened one to minimize

* Corresponding author.

E-mail address: zhangk826@163.com (K. Zhang).

system energy. The emission signal is usually weak because the excited state corresponds to a charge-transfer process which suffers badly from geometric relaxation and non-radiative decay. Except for this geometric relaxation which decreases system energy and increases non-radiative decay, solvent attack also helps to complete the non-radiative transformation from excited state to ground state. This quenching mechanism has been firstly reported by McMillin and coworkers, and then many following reports have proved its correctness [3–8].

In order to suppress this exciplex quenching, emitting system with mixed ligands have been proposed since they own long excited state lifetimes in solid state and degassed solutions [7,8]. For example, luminescent Cu(I) complexes with a typical molecular formula of $[\text{Cu}(\text{N}-\text{N})(\text{POP})]^+$ where POP = bis(2-(diphenylphosphanyl)phenyl) ether have been explored as promising emitters. The introduction of POP ligand is found to be efficient to block the solvent attack and geometric relaxation that occurs in excited state [9]. Theoretical analysis on $[\text{Cu}(\text{N}-\text{N})(\text{POP})]^+$ suggests that the steric effect of POP ligand is the key factor blocking excited state close to ground state [10]. It is also found that the highest occupied molecular orbital (HOMO) of $[\text{Cu}(\text{N}-\text{N})(\text{POP})]^+$ owns a predominant metal Cu d character, while, the lowest unoccupied orbital (LUMO) is essentially π^* orbital of diamine ligand. The emission corresponds to the radiative decay of the lowest triplet state and is thus assigned as a character of metal-to-ligand-charge-transfer $^3\text{MLCT}$ [$d(\text{Cu}) \rightarrow \pi^*(\text{diamine ligand})$]. The photophysical character of $[\text{Cu}(\text{N}-\text{N})(\text{POP})]^+$ excited state can be modified by changing ligand structures.

In this paper, we report six phosphorescent Cu(I) complexes with 1,10-phenanthroline-derived ligands and phosphorous ligands, including their synthesis, crystal structures, photophysical properties, and electronic nature. The correlation between ligand structure and photophysical properties of their corresponding Cu(I) complexes is studied in detail.

Experimental section

The molecular structures of the six Cu(I) complexes are shown in Scheme 1.

1,10-phenanthroline (referred to as Phen), 2,9-dimethyl-1,10-phenanthroline (referred to as DMPhen), Cu(BF₄)₂, bis(2-(diphenylphosphanyl)phenyl) ether (referred to as POP), triphenylphosphane (referred to as PPh₃), polyvinylpyrrolidone (PVP), polymethyl methacrylate (PMMA), and 2-cyanopyridine were purchased from Aldrich Chemical Co. and used without further purifications. The starting materials of $[\text{Cu}(\text{CH}_3\text{CN})_4]\text{BF}_4$ and 2,9-dibutyl-1,10-phenanthroline (referred to as DBPhen) were synthesized according to the literature procedures [7,11]. All organic solvents were purified using standard procedures.

Synthesis of Cu(I) complexes

All the Cu(I) complexes were synthesized according to the classic literature procedure [7]. Their identity was confirmed by ¹H NMR, ¹³C NMR elemental analysis, and single crystal XRD.

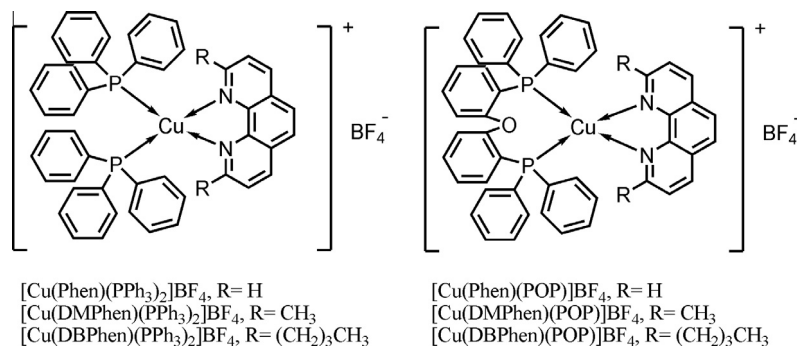
$[\text{Cu}(\text{Phen})(\text{PPh}_3)_2]\text{BF}_4$: 1.0 mmol of $[\text{Cu}(\text{CH}_3\text{CN})_4]\text{BF}_4$ and 2.0 mmol of PPh₃ were dissolved in 10 mL of CH₂Cl₂. The mixture was refluxed for 30 min at room temperature. Then 1.0 mmol of Phen was added. The mixture was refluxed for another half hour. The solvent was removed by rotary evaporation. The crude product was further purified by recrystallization from the mixed solvent of tetrahydrofuran/ether. Yield: 85%. ¹H NMR (CDCl₃, 300 MHz): 8.67 (2H, dd, *J* = 1.4 Hz, *J* = 4.6 Hz), 8.56 (2H, dd, *J* = 1.0 Hz, *J* = 9.0 Hz), 8.03 (2H, s), 7.78 (2H, q, *J* = 5.3 Hz), 7.33–7.27 (6H, m), 7.14 (12H, t, *J* = 8.6 Hz), 7.06–7.03 (12H, m). ¹³C NMR (CDCl₃, 75 MHz): 149.6, 143.1, 138.1, 132.9, 130.2, 129.7, 128.8, 127.4, 125.2. Anal. Calcd. for C₄₈H₃₈BCuF₄N₂P₂: C, 67.42; H, 4.48; N, 3.28. Found: C, 67.49; H, 4.37; N, 3.17.

$[\text{Cu}(\text{DMPhen})(\text{PPh}_3)_2]\text{BF}_4$: $[\text{Cu}(\text{DMPhen})(\text{PPh}_3)_2]\text{BF}_4$ was synthesized by a method similar to that of $[\text{Cu}(\text{Phen})(\text{PPh}_3)_2]\text{BF}_4$, except that Phen was replaced by DMPhen. Yield: 80%. ¹H NMR (CDCl₃, 300 MHz): 8.46 (2H, d, *J* = 9.2 Hz), 8.01 (2H, s), 7.51 (2H, d, *J* = 9.3 Hz), 7.36–7.31 (6H, m), 7.18–7.08 (24H, m), 2.14 (6H, s). ¹³C NMR (CDCl₃, 75 MHz): δ 159.1, 142.8, 138.4, 133.0, 132.1, 130.3, 128.6, 128.0, 126.3, 125.5, 27.1. Anal. Calcd. for C₅₀H₄₂BCuF₄N₂P₂: C, 68.00; H, 4.79; N, 3.17. Found: C, 68.12; H, 4.69; N, 3.08.

$[\text{Cu}(\text{DBPhen})(\text{PPh}_3)_2]\text{BF}_4$: $[\text{Cu}(\text{DBPhen})(\text{PPh}_3)_2]\text{BF}_4$ was synthesized by a method similar to that of $[\text{Cu}(\text{Phen})(\text{PPh}_3)_2]\text{BF}_4$, except that Phen was replaced by DBPhen. Yield: 81%. ¹H NMR (CDCl₃, 300 MHz): 8.54 (2H, d, *J* = 9.4 Hz), 8.06 (2H, s), 7.54 (2H, d, *J* = 9.4 Hz), 7.37–7.32 (6H, m), 7.21–7.11 (24H, m), 2.46 (4H, t, *J* = 9.3 Hz), 1.02–0.93 (4H, m), 0.68–0.61 (4H, m), 0.56 (6H, t, *J* = 7.5 Hz). Anal. Calcd. for C₅₆H₅₄BCuF₄N₂P₂: C, 69.53; H, 5.63; N, 2.90. Found: C, 69.77; H, 5.43; N, 2.75.

$[\text{Cu}(\text{Phen})(\text{POP})]\text{BF}_4$: $[\text{Cu}(\text{Phen})(\text{POP})]\text{BF}_4$ was synthesized by a method similar to that of $[\text{Cu}(\text{Phen})(\text{PPh}_3)_2]\text{BF}_4$, except that 2.0 mmol of PPh₃ was replaced by 1.0 mmol of POP. Yield: 82%. ¹H NMR (CDCl₃, 300 MHz): 8.72 (2H, d, *J* = 5.0 Hz), 8.50 (2H, d, *J* = 8.7 Hz), 8.01 (2H, s), 7.71 (2H, q, *J* = 5.3 Hz), 7.31 (2H, dt, *J* = 1.7 Hz, *J* = 8.6 Hz), 7.25–7.20 (4H, m), 7.10 (8H, t, *J* = 8.3 Hz), 7.05–6.92 (12H, m), 6.81–6.76 (2H, m). ¹³C NMR (CDCl₃, 75 MHz): 158.3, 149.5, 143.1, 137.5, 134.2, 132.8, 132.1, 130.5, 130.0, 129.5, 128.6, 127.2, 125.1, 124.1, 120.3. Anal. Calcd. for C₄₈H₃₆BCuF₄N₂OP₂: C, 66.33; H, 4.18; N, 3.22. Found: C, 66.20; H, 4.11; N, 3.12.

$[\text{Cu}(\text{DMPhen})(\text{POP})]\text{BF}_4$: $[\text{Cu}(\text{DMPhen})(\text{POP})]\text{BF}_4$ was synthesized by a method similar to that of $[\text{Cu}(\text{DMPhen})(\text{PPh}_3)_2]\text{BF}_4$, except that 2.0 mmol of PPh₃ was replaced by 1.0 mmol of POP. ¹H NMR (CDCl₃, 300 MHz): 8.37 (2H, d, *J* = 9.2 Hz), 7.85 (2H, s), 7.61 (2H, d, *J* = 9.2 Hz), 7.32 (2H, dt, *J* = 2.2 Hz, *J* = 8.6 Hz), 7.24–7.15 (8H,



Scheme 1. The molecular structures of the six Cu(I) complexes.

Table 1
Selected bond lengths (Å) and angles (°) of the three Cu(I) complexes.

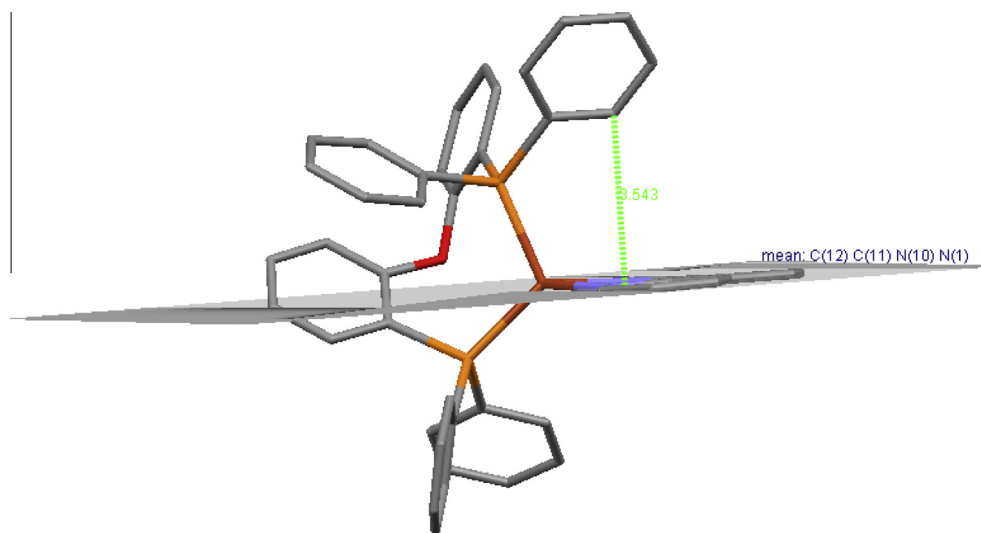
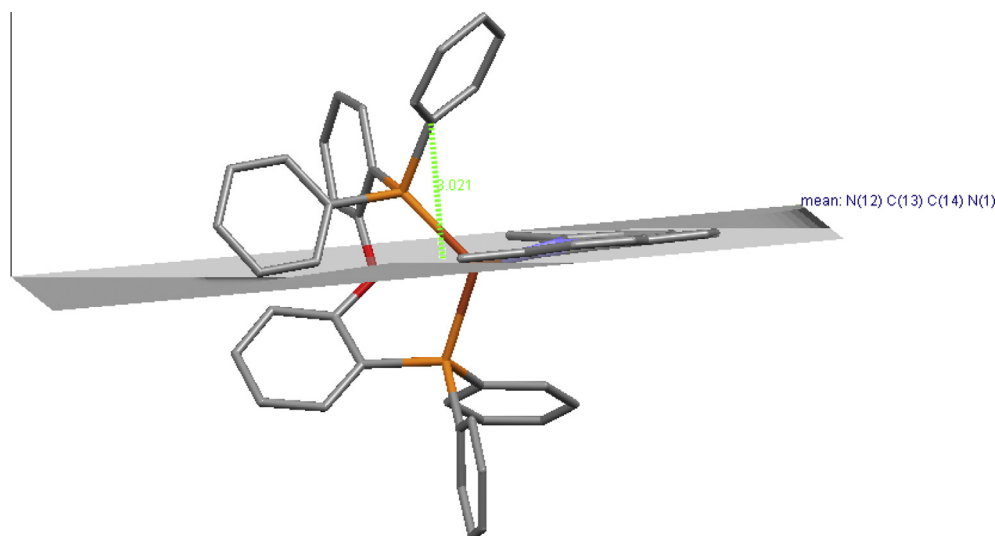
	[Cu(N-N)(POP)]BF ₄ , N-N =		
	Phen	DMPHEN	DBPhen
Cu(1)–N(1)	2.071	2.104	2.097
Cu(1)–N(2)	2.063	2.084	2.109
Cu(1)–P(1)	2.231	2.269	2.271
Cu(1)–P(2)	2.261	2.273	2.279
Cu···O	3.205	3.151	3.257
N(1)–Cu–N(2)	80.83	80.89	80.51
N(1)–Cu–P(1)	118.38	115.22	121.44
N(2)–Cu–P(1)	125.75	110.00	111.58
N(1)–Cu–P(2)	108.12	107.76	105.45
N(2)–Cu–P(2)	109.08	121.43	121.74
P(1)–Cu–P(2)	110.81	116.44	112.91

m), 7.01 (8H, t, $J = 8.3$ Hz), 6.97–6.91 (10H, m), 2.43 (6H, s). ¹³C NMR (CDCl₃, 75 MHz): δ 159.1, 158.3, 143.1, 138.0, 133.7, 132.7, 132.2, 131.6, 129.8, 128.4, 127.6, 126.0, 125.5, 125.3, 125.2, 120.0, 27.0. Anal. Calcd. for C₅₀H₄₀BCuF₄N₂OP₂: C, 66.94; H, 4.49; N, 3.12. Found: C, 66.73; H, 4.37; N, 3.04.

[Cu(DBPhen)(POP)]BF₄·[Cu(DBPhen)(POP)]BF₄ was synthesized by a method similar to that of [Cu(DBPhen)(PPh₃)₂]BF₄, except that 2.0 mmol of PPh₃ was replaced by 1.0 mmol of POP. ¹H NMR (CDCl₃, 300 MHz): 8.45 (2H, d, $J = 9.4$ Hz), 7.91 (2H, s), 7.64 (2H, d, $J = 9.4$ Hz), 7.35–7.28 (2H, m), 7.21–7.17 (8H, m), 7.01 (8H, t, $J = 8.2$ Hz), 6.96–6.90 (10H, m), 2.82 (4H, t, $J = 9.2$ Hz), 1.31–1.17 (4H, m), 0.76–0.65 (4H, m), 0.60 (6H, t, $J = 7.5$ Hz). ¹³C NMR (CDCl₃, 75 MHz): 162.6, 158.1, 142.8, 138.1, 133.4, 132.8, 132.0, 131.4, 129.8, 128.4, 128.1, 126.1, 125.3, 125.0, 123.3, 120.1, 40.6, 30.4, 22.1, 13.7. Anal. Calcd. for C₅₆H₅₂BCuF₄N₂OP₂: C, 68.54; H, 5.34; N, 2.85. Found: C, 68.46; H, 5.22; N, 2.79.

Methods and measurements

Density functional theory (DFT) and singlet excitation calculations using time-dependent density functional theory (TD-DFT) were performed on the Cu(I) complexes at RB3PW91/SBKJC level [12], and at RB3LYP/SBKJC level for comparison (see Supporting information for details). The initial geometries were obtained from their single crystal structures. All computations were finished by GAMESS software package. The graphical presentation was

**Fig. 1A.** Molecular structure of [Cu(Phen)(POP)]BF₄, showing the interaction between phenyl ring from POP and Phen. BF₄⁻ and hydrogen atoms are not shown for clarity.**Fig. 1B.** Molecular structure of [Cu(DMPHEN)(POP)]BF₄, showing the interaction between phenyl ring from POP and DMPHEN. BF₄⁻ and hydrogen atoms are not shown for clarity.

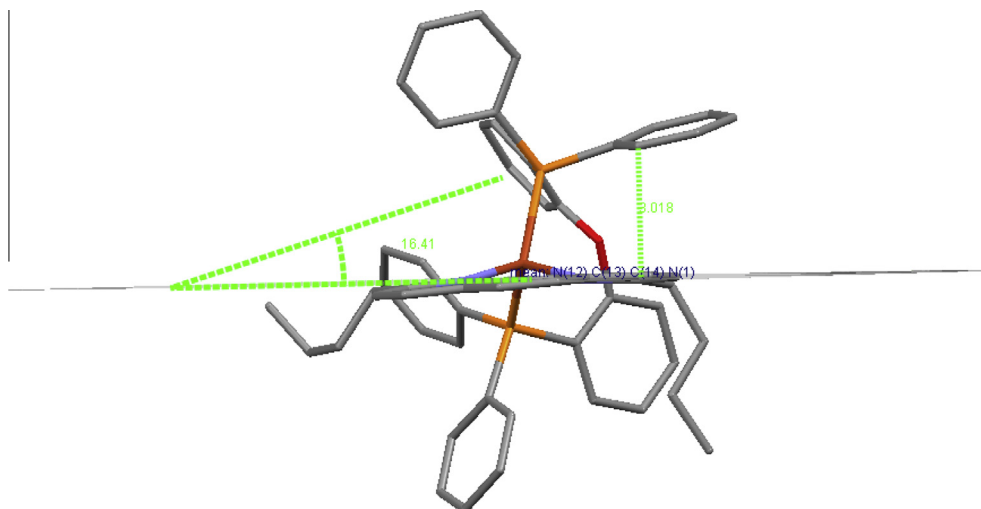


Fig. 1C. Molecular structure of $[\text{Cu}(\text{DBPhen})(\text{POP})]\text{BF}_4$, showing the interaction between phenyl ring from POP and DBPhen. BF_4^- and hydrogen atoms are not shown for clarity.

Table 2
Summarized photophysical parameters of the six Cu(I) complexes.

$[\text{Cu}(\text{N}-\text{N})(\text{P}-\text{P})]\text{BF}_4$ N-N, P-P =	$\lambda_{\text{abs}}^{\text{a}}$ (nm)	$\lambda_{\text{em}}^{\text{a}}$ (nm)	Φ^{b}	τ^{c} (μs)	K_{r} ($\times 10^4 \text{ s}^{-1}$)	K_{nr} ($\times 10^4 \text{ s}^{-1}$)
Phen, $(\text{PPh}_3)_2$	368	541	0.13	8.2	1.58	10.61
DMPhen, $(\text{PPh}_3)_2$	365	510	0.35	18.4	1.90	3.53
DBPhen, $(\text{PPh}_3)_2$	363	504	0.56	33.1	1.69	1.33
Phen, POP	395	556	0.15	4.5	3.33	18.89
DMPhen, POP	385	527	0.50	13.3	3.76	3.76
DBPhen, POP	381	518	0.70	20.5	3.41	1.47

^a ± 1 nm.

^b $\pm 10\%$, Measured according to the literature method of Ref. [9].

^c $\pm 5\%$, $I = A_1 \exp(-t/\tau_1) + A_2 \exp(-t/\tau_2)$, $\tau = (A_1 \tau_1^2 + A_2 \tau_2^2) / (A_1 \tau_1 + A_2 \tau_2)$.

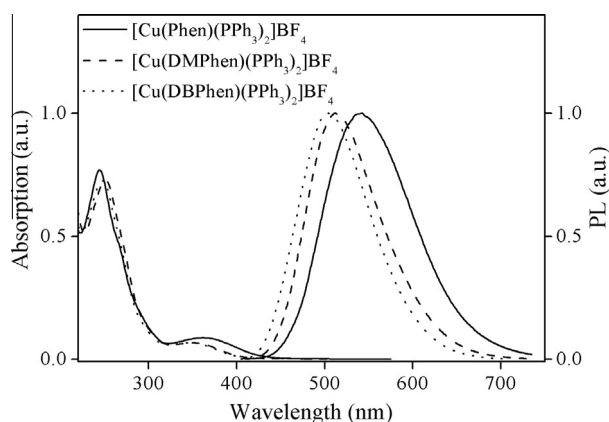


Fig. 2A. UV-Vis absorption and PL spectra of $[\text{Cu}(\text{N}-\text{N})(\text{PPh}_3)_2]\text{BF}_4$, where N-N = Phen, DMPhen, and DBPhen.

generated by wxMacmolplt software package with contour value of 0.025.

Excited state lifetimes were obtained with a 355 nm light generated from the third-harmonic-generator pump, using pulsed Nd:YAG laser as the excitation source. The Nd:YAG laser possesses a line width of 1.0 cm^{-1} , pulse duration of 10 ns, and repetition frequency of 10 Hz. A Rhodamine 6G dye pumped by the same Nd:YAG laser was used as the frequency-selective excitation source. All PL spectra were measured with a Hitachi F-4500

fluorescence spectrophotometer. Solid state photoluminescence quantum yields were measured with the Hitachi F-4500 fluorescence spectrophotometer equipped with an integrating sphere [9]. UV-Vis absorption spectra were recorded using a Shimadzu UV-3101PC spectrophotometer. ^1H NMR spectra were obtained with a Varian INOVA 300 spectrometer. Elemental analysis was performed on a Carlo Erba 1106 elemental analyzer. Single crystal data were collected on a Siemens P4 single-crystal X-ray diffractometer with a Smart CCD-1000 detector and graphite-monochromated

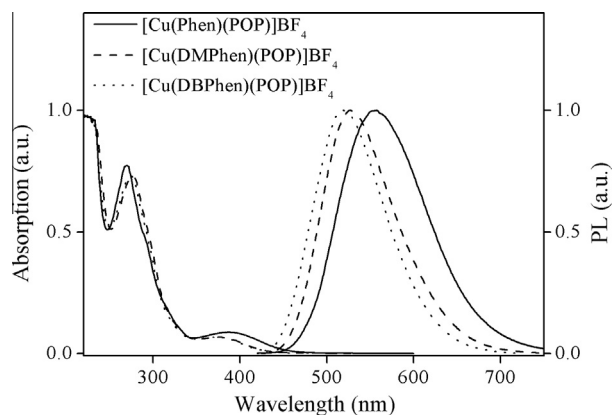


Fig. 2B. UV-Vis absorption and PL spectra of $[\text{Cu}(\text{N}-\text{N})(\text{POP})]\text{BF}_4$, where N-N = Phen, DMPhen, and DBPhen.

Mo $K\alpha$ radiation, operating at 50 kV and 30 A at 298 K. All hydrogen atoms were calculated. All data were recorded using single crystal samples in the air at room temperature without being specified.

Results and discussion

Single crystal structures

The crystal structures of $[\text{Cu}(\text{Phen})(\text{POP})]\text{BF}_4$, $[\text{Cu}(\text{DMPhen})(\text{POP})]\text{BF}_4$, and $[\text{Cu}(\text{DBPhen})(\text{POP})]\text{BF}_4$ are observed, and the selected geometric parameters are listed in Table 1. The Cu(I) center in the three complexes has a distorted tetrahedral geometry. The dihedral angles between N–Cu–N and P–Cu–P planes for the three complexes are measured to be 88.36° for $[\text{Cu}(\text{Phen})(\text{POP})]\text{BF}_4$, 82.33° for $[\text{Cu}(\text{DMPhen})(\text{POP})]\text{BF}_4$, and 78.80° for $[\text{Cu}(\text{DBPhen})(\text{POP})]\text{BF}_4$, respectively. The Cu–N bond

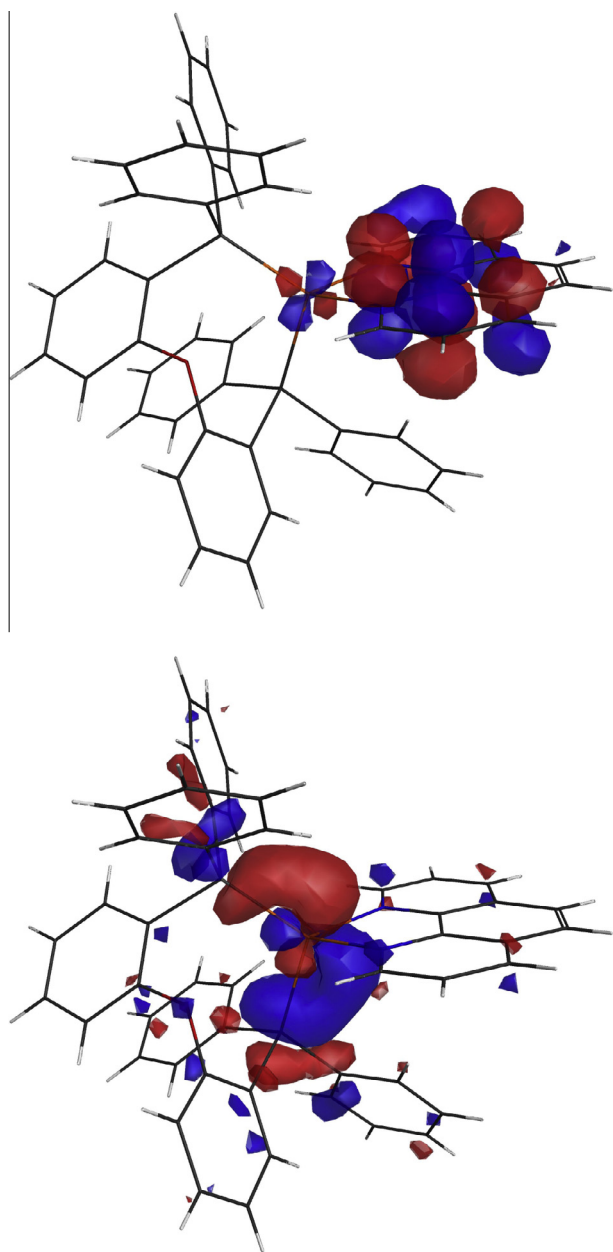


Fig. 3A. HOMO (down) and LUMO (up) of $[\text{Cu}(\text{Phen})(\text{POP})]^+$.

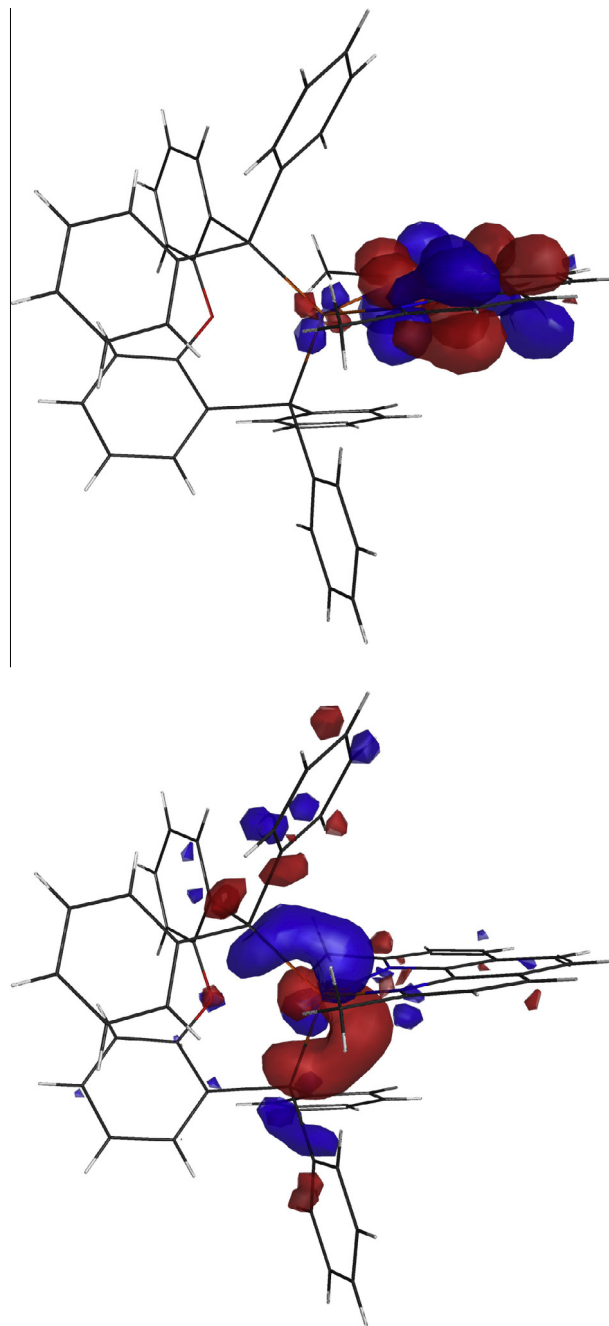


Fig. 3B. HOMO (down) and LUMO (up) of $[\text{Cu}(\text{DMPhen})(\text{POP})]^+$.

length of the three Cu(I) complexes increases with the increasing alkyl steric hindrance. Above results suggest that the introduction of alkyl chain into 2,9-positions of 1,10-phenanthroline leads to a crowded coordination sphere around Cu(I) center, and the Cu(I) center tries to minimize the congestion by extending Cu–N bond and decreasing the dihedral angle between N–Cu–N and P–Cu–P planes.

On the other hand, Cu–P bond lengths of the three Cu(I) complexes are similar to each other, showing no response towards the introduction of alkyl chain. The oxygen atom of POP ligand in the three Cu(I) complexes localizes at a distance of ~ 3.2 Å away from the Cu(I) center and opposite to the coordinated N atoms, indicating a weak interaction between oxygen atom and Cu(I) center. Similar Cu \cdots O separations have also been reported in POP-based Cu(I) complexes [10,13].

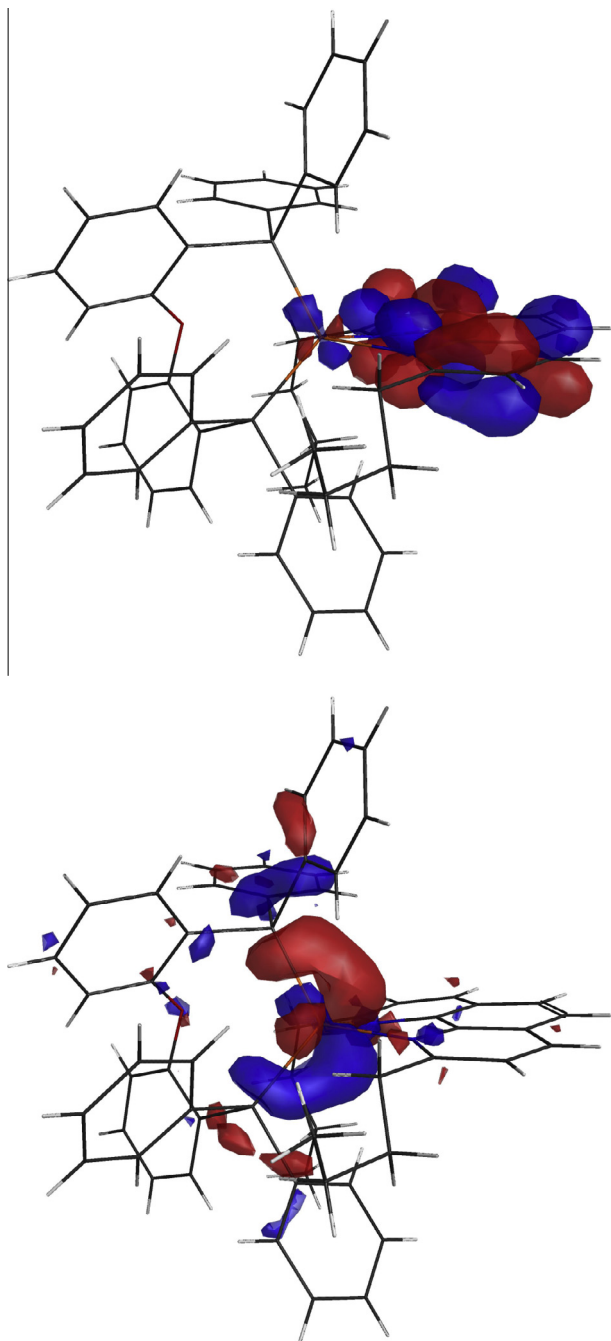


Fig. 3C. HOMO (down) and LUMO (up) of $[\text{Cu}(\text{DBPhen})(\text{POP})]^+$.

N–Cu–N bond angles of the three Cu(I) complexes are quite similar to each other ($\sim 80^\circ$) with small variations, which means that the bite angles in Phen-derived ligands are nearly invariable. In contrast, P–Cu–P bond angle varies dramatically from 110.81° for $[\text{Cu}(\text{Phen})(\text{POP})]\text{BF}_4$ to 116.44° for $[\text{Cu}(\text{DM})(\text{POPh})]\text{BF}_4$ as shown in Table 1. Considering POP's natural bite angle of 102.2° , with a flexibility range from 86° to 120° , the large P–Cu–P bond angles suggest a crowded coordination environment around Cu(I) center, which is consistent with above analysis [14].

It is also observed from their molecular structures that the interaction between phenyl ring from POP and Phen-derived ligands increases with the increasing alkyl steric hindrance. As shown in Fig. 1, in $[\text{Cu}(\text{Phen})(\text{POP})]\text{BF}_4$, the minimum distance between phenyl ring from POP and diamine ligand is 3.543 \AA , the corresponding value for $[\text{Cu}(\text{DMPhen})(\text{POP})]\text{BF}_4$ decreases to

3.021 \AA . As for $[\text{Cu}(\text{DBPhen})(\text{POP})]\text{BF}_4$ which owns the most intense steric hindrance, large P–Cu–P bond angle of $[\text{Cu}(\text{DBPhen})(\text{POP})]\text{BF}_4$ allows one of POP's phenyl ring to align almost parallel to DBPhen ring so that their mean planes intersect with an angle of 16.41° , and the minimum distance between phenyl ring from POP and diamine ligand is only 3.018 \AA . As above mentioned, the excited state Cu(I) center tends to waste its energy by switching its coordination sphere from a tetragonally flattened one to a tetrahedral-like one, this interaction between phenyl ring from POP and diamine ligand may effectively block the geometry transition, leading to improved photophysical performances, which will be discussed below.

Photophysical properties

The photophysical parameters of the six Cu(I) complexes dispersed in PMMA films (10 wt%) are summarized in Table 2. Fig. 2 shows the UV–Vis absorption spectra of the six Cu(I) complexes in CH_2Cl_2 solutions with a concentration of $1 \times 10^{-5} \text{ mol/L}$. It can be observed that the spectral band shapes are quite similar to each other due to their similar diimine and phosphorous ligands. Each absorption spectrum is typically composed of a high-energy absorption band ranging from 350 nm to 220 nm and a low-energy absorption band ranging from 350 nm to 500 nm. The former one corresponds to ligands $\pi \rightarrow \pi^*$ transitions according to literature reports [9,10,13]. While, the latter one is experimentally assigned as MLCT transition absorption. Compared with the absorption spectrum of $[\text{Cu}(\text{Phen})(\text{POP})]\text{BF}_4$, it can be seen that the introduction of alkyl chain into 2,9-positions of 1,10-phenanthroline leads to a blue shift to the absorption spectra of corresponding $[\text{Cu}(\text{N–N})(\text{POP})]\text{BF}_4$ complexes, where N–N = DMPhen and DBPhen [9]. In addition, $[\text{Cu}(\text{N–N})(\text{PPh}_3)_2]\text{BF}_4$ need more energy for onset electronic transition compared with $[\text{Cu}(\text{N–N})(\text{POP})]\text{BF}_4$, where N–N = Phen, DMPhen, and DBPhen.

As shown in Fig. 2, the six Cu(I) complexes exhibit broad emission spectra (λ_{em}) at room temperature, and their emission peaks are listed in Table 2. Those emissions render no vibronic progressions, indicating that the excited states own a CT character. Large Stokes shifts between absorption peaks (λ_{abs}) and emission peaks (λ_{em}) are observed for the Cu(I) complexes (173 nm for $[\text{Cu}(\text{Phen})(\text{PPh}_3)_2]\text{BF}_4$, 145 nm for $[\text{Cu}(\text{DMPhen})(\text{PPh}_3)_2]\text{BF}_4$, and 141 nm for $[\text{Cu}(\text{DBPhen})(\text{PPh}_3)_2]\text{BF}_4$, while 161 nm for $[\text{Cu}(\text{Phen})(\text{POP})]\text{BF}_4$, 142 nm for $[\text{Cu}(\text{Phen})(\text{POP})]\text{BF}_4$, and 137 nm for $[\text{Cu}(\text{DBPhen})(\text{POP})]\text{BF}_4$). Those large Stokes shifts reveal that the six Cu(I) complexes experience intense geometric relaxation in excited state, and this geometric relaxation tends to become weak with the increasing increasing alkyl steric hindrance from Phen to DBPhen.

The PL quantum yields (Φ) for the six Cu(I) complexes are measured, along with their PL decay lifetimes (τ), as shown in Table 2. Their phosphorescent nature can be confirmed by the long-lived excited state. It is notable that both PL quantum yield and PL decay lifetime tend to increase with the increasing alkyl steric hindrance from Phen to DBPhen, which means that luminescence is greatly enhanced by the introduction of alkyl chain into 2,9-positions of 1,10-phenanthroline. Based on the quantum yields and lifetime data on hand, the radiative probability and nonradiative probability values, K_r and K_{nr} , are calculated with (1) and (2) as follows:

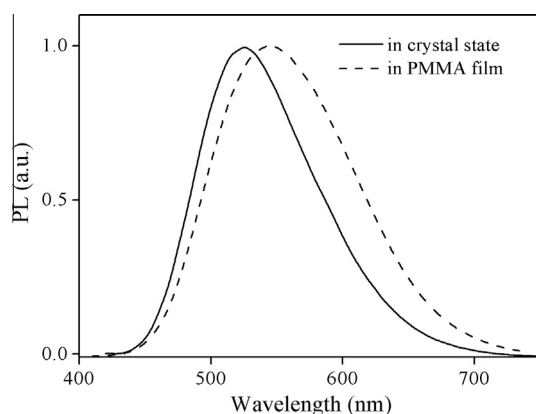
$$\Phi = \frac{K_r}{K_r + K_{nr}} \quad (1)$$

$$\frac{1}{\tau} = K_r + K_{nr} \quad (2)$$

As shown in Table 2, the radiative probability values of $[\text{Cu}(\text{N–N})(\text{POP})]\text{BF}_4$ are typically two times bigger than $[\text{Cu}(\text{N–N})(\text{PPh}_3)_2]\text{BF}_4$, where N–N = Phen, DMPhen, and DBPhen. On the other hand,

Table 3Calculated percentage composition of the first five singlet excitations of $[\text{Cu}(\text{N-N})(\text{POP})]^+$ calculated at RB3PW91/SBKJC level.

	$[\text{Cu}(\text{N-N})(\text{POP})]^+$, N-N =		
	Phen	DMPHEN	DBPhen
$S_0 \rightarrow S_1$	HOMO \rightarrow LUMO(91.7%) 460.04 nm	HOMO \rightarrow LUMO(75.5%) 435.79 nm	HOMO \rightarrow LUMO(89.1%) 449.18 nm
$S_0 \rightarrow S_2$	HOMO \rightarrow LUMO+1(97.3%) 451.40 nm	HOMO-1 \rightarrow LUMO(72.5%) 407.21 nm	HOMO \rightarrow LUMO+1(93.3%) 406.82 nm
$S_0 \rightarrow S_3$	HOMO-1 \rightarrow LUMO(90.4%) 447.81 nm	HOMO \rightarrow LUMO+1(93.1%) 402.48 nm	HOMO-1 \rightarrow LUMO(85.6%) 399.79 nm
$S_0 \rightarrow S_4$	HOMO-1 \rightarrow LUMO+1(88.3%) 410.11 nm	HOMO-2 \rightarrow LUMO(94.4%) 385.21 nm	HOMO-2 \rightarrow LUMO(95.8%) 375.49 nm
$S_0 \rightarrow S_5$	HOMO-2 \rightarrow LUMO(83.9%) 404.66 nm	HOMO-1 \rightarrow LUMO+1(93.9%) 371.49 nm	HOMO-1 \rightarrow LUMO+1(95.8%) 359.17 nm

**Fig. 4.** PL spectrum of $[\text{Cu}(\text{Phen})(\text{PPh}_3)_2]\text{BF}_4$ in crystal state and in PMMA film.

the nonradiative probability values of $[\text{Cu}(\text{N-N})(\text{POP})]\text{BF}_4$ and $[\text{Cu}(\text{N-N})(\text{PPh}_3)_2]\text{BF}_4$ decrease dramatically with the increasing alkyl steric hindrance from Phen to DBPhen. Thus, we come to a conclusion that the introduction of alkyl chain into 2,9-positions of 1,10-phenanthroline effectively suppresses K_{nr} decay process, leading to the luminescence enhancement.

Theoretical calculations

As mentioned, the emissive state of phosphorescent Cu(I) complexes is usually affected by both ligand electronic nature and coordination geometry. In order to confirm that the luminescence enhancement is caused by the steric hindrance effect, instead of electronic effect, we perform a DFT/TD-DFT calculation, which has been proved to be a powerful tool to investigate electronic properties of transition metal complexes, on $[\text{Cu}(\text{N-N})(\text{POP})]^+$ at RB3PW91/SBKJC level, where N-N = Phen, DMPHEN, and DBPhen [10].

As shown in Fig. 3, the highest occupied molecular orbitals (HOMOs) of $[\text{Cu}(\text{N-N})(\text{POP})]^+$ have an evident metal Cu character, admixed with large contributions from the phosphorous ligand of POP, while, the lowest unoccupied molecular orbitals (LUMOs) of $[\text{Cu}(\text{N-N})(\text{POP})]^+$ are essentially diimine ligand π^* orbital of Phen. The calculated onset transitions correspond to an electronic transition from HOMO to LUMO, and the onset excitation energy values listed in Table 3 correlates quite well with the experimentally recorded absorption edge shown in Fig. 2. It is thus confirmed that the onset electronic transition of $[\text{Cu}(\text{N-N})(\text{POP})]^+$ is a MLCT one. Correspondingly, the emissive state of $[\text{Cu}(\text{N-N})(\text{POP})]^+$ which derives from onset electronic excitation is also a MLCT one. Combined with the long excited state lifetimes as mentioned, we come to a conclusion that the emissions of $[\text{Cu}(\text{N-N})(\text{POP})]\text{BF}_4$ originate from

$^3\text{MLCT}$ excited states, showing no luminescence mechanism difference. Consequently, the luminescence enhancement with increasing alkyl steric hindrance is not caused by their electronic nature difference.

Further confirmation on luminescence enhancement

In order to further confirm that the luminescence enhancement is triggered by the increasing alkyl steric hindrance, we compare the photophysical properties of $[\text{Cu}(\text{Phen})(\text{PPh}_3)_2]\text{BF}_4$ in crystal state and in PMMA film. As shown in Fig. 4, the PL spectrum of crystal $[\text{Cu}(\text{Phen})(\text{PPh}_3)_2]\text{BF}_4$ peaks at 522 nm, compared with 541 nm from $[\text{Cu}(\text{Phen})(\text{PPh}_3)_2]\text{BF}_4$ doped PMMA film. In addition, the crystal sample exhibits a much higher PL quantum yield of 0.75, compared with 0.13 from $[\text{Cu}(\text{Phen})(\text{PPh}_3)_2]\text{BF}_4$ doped PMMA film. It is observed that the PL performances of $[\text{Cu}(\text{Phen})(\text{PPh}_3)_2]\text{BF}_4$ in crystal state is much superior to those in dispersed film, which can be explained as follows.

McMillin and coworker's reports confirm that the dominant nonradiative decay process is the geometric relaxation that occurs at excited state from a tetragonally flattened geometry to a tetrahedral-like one [3,5–7]. According to Zhang and coworkers, there exists face-to-face pi-pi stacking in crystal state $[\text{Cu}(\text{Phen})(\text{PPh}_3)_2]\text{BF}_4$ which is believed to be a partially rigid structure. Thus, it is expected that this geometric relaxation is somehow suppressed by the rigid environment, resulting in the enhanced luminescence of $[\text{Cu}(\text{Phen})(\text{PPh}_3)_2]\text{BF}_4$ in crystal state [15]. After being dispersed in PMMA film, the rigid environment around $[\text{Cu}(\text{Phen})(\text{PPh}_3)_2]\text{BF}_4$ molecules is expected to be destroyed. The alkyl moieties at 2,9-positions of 1,10-phenanthroline should be the only reason for improved PL performance. In other words, their steric effect effectively limits the excited state geometric relaxation, showing better PL performance.

Conclusion

In this paper, we report six phosphorescent Cu(I) complexes with 1,10-phenanthroline-derived ligands and phosphorous ligands, including their synthesis, crystal structures, photophysical properties, and electronic nature. The Cu(I) center has a distorted tetrahedral geometry within the Cu(I) complexes. Theoretical calculation reveals that all emissions originate from triplet metal-to-ligand-charge-transfer excited state. The correlation between ligand structure and photophysical properties of their corresponding Cu(I) complexes is studied in detail. It is found that the introduction of alkyl moieties into 2,9-positions of 1,10-phenanthroline is highly effective on restricting the geometric relaxation that occurs in excited states, which greatly enhances the PL performances, including PL quantum yield improvement, PL decay lifetime increase, and emission blue shift. This finding

may be useful when designing high-performance phosphorescent Cu(I) complexes.

Acknowledgments

The authors gratefully thank the support and help from The Central Institute for Correctional Police, Academic innovation team of young teachers 2012.

Appendix A. Supplementary material

Supplementary data associated with this article can be found, in the online version, at <http://dx.doi.org/10.1016/j.saa.2014.01.019>.

References

- [1] K.E. Erkkila, D.T. Odom, J.K. Barton, *Chem. Rev.* 99 (1999) 2777–2796.
- [2] C.A. Bigozzi, R. Argazzi, C.J. Kleverlaan, *Chem. Soc. Rev.* 29 (2000) 87–96.

- [3] D.R. McMillin, K.M. McNett, *Chem. Rev.* 98 (1998) 1201–1209.
- [4] N. Armaroli, *Chem. Soc. Rev.* 30 (2001) 113–124.
- [5] L. Zhang, S. Yue, B. Li, D. Fan, *Inorg. Chim. Acta* 384 (2012) 225–232.
- [6] T. Cunningham, K.L.H. Cunningham, J.F. Michalec, D.R. McMillin, *Inorg. Chem.* 38 (1999) 4388–4392.
- [7] D.G. Cuttall, S.M. Kuang, P.E. Fanwick, D.R. McMillin, R.A. Walton, *J. Am. Chem. Soc.* 124 (2002) 6–7.
- [8] R.A. Rader, D. McMillin, M.T. Buckner, T.G. Matthews, D.J. Casadonte, R.K. Lengel, S.B. Whittaker, L.M. Darmon, F.E. Lytle, *J. Am. Chem. Soc.* 103 (1981) 5906–5912.
- [9] Q. Zhang, Q. Zhou, Y. Cheng, L. Wang, D. Ma, X. Jing, F. Wang, *Adv. Mater.* 16 (2004) 432–436.
- [10] L. Yang, J.K. Feng, A.M. Ren, M. Zhang, Y.G. Ma, X.D. Liu, *Eur. J. Inorg. Chem.* 10 (2005) 1867–1879.
- [11] L. Shi, B. Li, S. Yue, D. Fan, *Sensor Actuat. B Chem.* 137 (2009) 386–392.
- [12] K. Su, J. Wei, X. Hu, H. Yue, L. Lv, Y. Wang, Z. Wen, *Acta Phys. – Chim. Sin.* 16 (2000) 643–651.
- [13] S.M. Kuang, D.G. Cuttall, D.R. McMillin, P.E. Fanwick, R.A. Walton, *Inorg. Chem.* 41 (2002) 3313–3322.
- [14] M. Kranenburg, Y.E.M. van der Brugt, P.C.J. Kamer, P.W.N.M. van Leeuwen, *Organometallics* 14 (1995) 3081–3089.
- [15] L. Zhang, B. Li, Z. Su, *Langmuir* 25 (2009) 2068–2074.